The function of melanotransferrin: a role in melanoma cell proliferation and tumorigenesis

L.L.Dunn[†], E.O.Sekyere[†], Y.Suryo Rahmanto and D.R.Richardson[1],*

Children's Cancer Institute Australia for Medical Research, Iron Metabolism and Chelation Program, P.O. Box 81, High Street, Randwick, Sydney, New South Wales, 2031 Australia and [1]The Heart Research Institute, 145 Missenden Road, Camperdown, Sydney, New South Wales, 2050 Australia

*To whom correspondence should be addressed at: Iron Metabolism and Chelation Program, Department of Pathology, University of Sydney, Sydney, New South Wales, 2006 Australia. Tel: +61-2-9036-6548; Fax: +61-2-9036-6549;
Email: d.richardson@pathology.usyd.edu.au

Melanotransferrin (MTf) or melanoma tumor antigen p97 is an iron (Fe) binding transferrin homolog expressed highly on melanomas and at lower levels on normal tissues. It has been suggested that MTf is involved in a variety of processes such as Fe metabolism and cellular differentiation. Considering the crucial role of Fe in many metabolic pathways, for example, DNA synthesis, it is important to understand the function of MTf. To define the roles of MTf, two models were developed: (i) an MTf knockout ($MTf^{-/-}$) mouse and (ii) downregulation of MTf expression in melanoma cells by post-transcriptional gene silencing (PTGS). Examination of the $MTf^{-/-}$ mice demonstrated no differences compared with wild-type littermates. However, microarray analysis showed differential expression of molecules involved in proliferation such as *Mef2a, Tcf4, Gls* and *Apod* in $MTf^{-/-}$ mice compared with $MTf^{+/+}$ littermates. Considering the role of MTf in melanoma cells, PTGS was used to downregulate *MTf* mRNA and protein levels by >90 and >80%, respectively. This resulted in inhibition of proliferation and migration. As found in $MTf^{-/-}$ mice, in melanoma cells with suppressed MTf expression, *hMEF2A* and *hTCF4* were upregulated compared with parental cells. Furthermore, when melanoma cells with decreased MTf expression were injected into nude mice, tumor growth was markedly reduced, suggesting a role for MTf in proliferation and tumorigenesis.

Introduction

Melanotransferrin (MTf) or melanoma tumor antigen p97 is an iron (Fe) binding transferrin (Tf) homolog originally

Abbreviations: ALP, alkaline phosphatase; Apod, apolipoprotein D; FAC, ferric ammonium citrate; Gls, glutaminase; hOAS, 2′,5′-oligoadenylate synthetase; Mef2a, myocyte enhancer factor 2A; MTf, melanotransferrin; MTf^{+/+}, wild-type MTf; MTf^{−/−}, MTf knockout; sMTf, soluble MTf; PTGS, post-transcriptional gene silencing; RT–PCR, reverse transcription–polymerase chain reaction; SD, standard deviation; SEM, standard error of the mean; Tcf4, transcription factor 4; Tf, transferrin; TfR1, Tf receptor 1; TIBC, total Fe-binding capacity.

[†]These authors contributed equally to this work.

identified at high levels on melanomas and other tumors, cell lines and fetal tissues (1–3). Initial studies found MTf to be absent or only slightly expressed in normal adult tissues (2), while later investigations demonstrated MTf in a range of normal tissues (4–6). Recent studies showed MTf to be expressed at higher levels in the brain and epithelial surfaces of the salivary gland, pancreas, testis, kidney and sweat gland ducts compared with other normal tissues (7–9). Nonetheless, the highest levels of MTf are found on melanoma cells, in particular the SK-Mel-28 melanoma cell line that expresses $3.0–3.8 \times 10^5$ MTf molecules per cell (2,3).

The MTf molecule shares many properties in common with the Tf family of proteins, including (i) a 37–39% sequence homology with human serum Tf, human lactoferrin and chicken ovoTf; (ii) co-localization of the *MTf* gene on chromosome 3 with *Tf* and the *Tf receptor 1* (*TfR1*) genes; (iii) many conserved disulfide bonds; (iv) an N-terminal Fe-binding site that is very similar to that found in serum Tf; and (v) the ability of isolated and purified MTf to bind Fe from Fe(III) citrate complexes (3,10–13). These characteristics and the high expression of MTf on melanoma cells suggested that it played a role in Fe transport, possibly assisting these tumor cells with their increased Fe requirements (7,14,15). However, unlike serum Tf, MTf is typically tethered to the cell membrane by a glycosyl phosphatidylinositol (GPI) anchor with only a very small amount of soluble MTf (sMTf) being detectable in serum, saliva, urine and cerebrospinal fluid (2,16,17).

Extensive *in vitro* studies examining the role of MTf in Fe uptake by SK-Mel-28 melanoma cells demonstrated that both the membrane-bound and soluble forms of MTf do not efficiently donate Fe to the cell, or bind to either TfR1 or transferrin receptor 2 (7,14,15,18–20). Analysis of normal tissues in humans and mice indicates that the expression pattern of MTf is very different to that of Tf and TfR1, and that MTf expression is not regulated by Fe levels (7). Collectively, these findings suggest that MTf has a negligible role in cellular Fe uptake in melanoma cells.

To date, the function of MTf in both normal and neoplastic cells remains unknown. A wide variety of studies have suggested that MTf is involved in physiological and pathological processes, such as (i) Fe transport (21,22); (ii) Alzheimer's disease (16,23); (iii) eosinophil differentiation (24); (iv) chondrogenesis (25); (v) arthritis (26); (vi) angiogenesis (27); and (vii) plasminogen activation (28). However, there is no definitive evidence for the functional role of MTf.

To determine the role of MTf, we generated MTf knockout ($MTf^{-/-}$) mice by targeted gene disruption. A preliminary report on this work described the development of this mouse model with very limited description of the effects of the null allele on Fe homeostasis (9). In the current paper, we provide a comprehensive assessment of the phenotype of this animal, which is important for defining the function of MTf. Our studies show that lack of MTf expression had no significant

effect on the growth, development, behavior or metabolism of $MTf^{-/-}$ mice compared with wild-type ($MTf^{+/+}$) littermates. However, whole genome microarray analysis showed changes in the expression of genes such as *myocyte enhancer factor 2A* (*Mef2a*), *transcription factor 4* (*Tcf4*), *glutaminase* (*Gls*) and *apolipoprotein D* (*Apod*) when comparing $MTf^{-/-}$ mice with $MTf^{+/+}$ littermates. To assess the role of MTf in neoplastic cells, we downregulated MTf expression by post-transcriptional gene silencing (PTGS) in SK-Mel-28 melanoma cells. These studies showed that downregulation of MTf expression impaired cellular proliferation, DNA synthesis, cellular migration *in vitro* and tumor formation *in vivo*.

Materials and methods

Animals

$MTf^{-/-}$ mice were generated by homologous gene targeting in embryonic stem (ES) cells as described previously (9). Animal work was conducted in accordance with the University of New South Wales Animal Ethics Committee Guidelines. All mice were housed under a 12 h light–dark cycle, fed routinely with basal rodent chow (0.02% Fe) and watered *ad libitum*.

Serum chemistry, hematology and histochemistry

Serum chemistry and hematological parameters were determined using a Konelab 20i analyzer (Thermo-Electron Corporation, Finland) and Sysmex K-4500 analyzer (TOA Medical Electronics, Kobe, Japan), respectively. The total Fe-binding capacity (TIBC) was calculated by adding the serum Fe level and the unbound Fe-binding capacity (UIBC). The Tf saturation was calculated as serum Fe level/TIBC × 100.

Blood and bone marrow smears were prepared and stained with Giemsa. A wide variety of tissues were dissected, fixed in formalin, sectioned and stained with hematoxylin and eosin and Prussian blue. These were assessed by two independent veterinary pathologists.

Tissue non-heme Fe, copper and zinc determinations

Tissue non-heme Fe, copper (Cu) and zinc (Zn) concentrations were measured using inductively coupled plasma atomic emission spectrometry (ICP-AES) via standard techniques (29).

Microarray processing and analysis

Six 17.5-week-old female mice comprising four $MTf^{-/-}$ and two $MTf^{+/+}$ from the same litter were used. Total RNA was isolated by grinding brain tissue in 1 ml of TRIzol reagent (Invitrogen, Sydney, Australia). First-strand cDNA synthesis was performed using a total of 15 μg of RNA by the Affymetrix One Cycle cDNA synthesis kit and the cDNA products purified using the Affymetrix GeneChip sample clean-up kit (Millenium Sciences, Victoria, Australia). Using the Affymetrix IVT labeling kit (Millenium Sciences), biotin-labeled cRNA was prepared from the cDNA template. After further purification with the above-mentioned clean-up kit, the quantity of product was ascertained using the Nanochip protocol on an Agilent Bioanalyzer 2100

(Agilent Technologies, CA). A total of 20 μg of labeled cRNA was fragmented to the 50–200 bp size range and the quality of the fragments was checked again. Samples (cRNA, 0.05 μg/μl) that passed this checkpoint were then prepared for hybridization to the mouse GeneChip 430 2.0. The mouse GeneChip 430 2.0 consists of >39 000 transcripts and variants from >34 000 well-characterized mouse genes. On completion of hybridization and washing, microarray chips were scanned with the Affymetrix GeneChip Scanner 3000 (Millenium Sciences). Microarray data are available on the Gene Expression Omnibus (http://www.ncbi.nlm.nih.gov/geo/) using the accession numbers GSM101412, GSM101413, GSM101414, GSM101415, GSM101416 and GSM101417.

A two-phase strategy was used to identify differentially expressed genes. First, genome-wide screening was performed using Affymetrix GeneChips. The empirical Bayes procedure (30) was applied in order to detect genes most likely to be differentially expressed between the $MTf^{-/-}$ and $MTf^{+/+}$ samples. Individual *P*-values were then adjusted using the Holm step-down procedure to reduce the likelihood of false positives (31). Statistical analysis of data from the Affymetrix Genechips were used to produce a list of 30 genes with the greatest fold change. This analysis was not meant to provide proof of differential expression. Rather, definitive evidence of differential expression was obtained from the reverse transcription–polymerase chain reaction (RT–PCR) assessment of samples used for the microarray analysis and also at least three other independent samples.

Construction of siRNA vectors, cell culture and transfections

To prepare a construct capable of generating hairpin siRNA specific for human *MTf* mRNA, we used the expression vector, p*Silencer* 3.1-H1 neo (Ambion, Texas). The vector was used to clone four separate transgenes (A–D) of 66 bp each that transcribe 19mer double-stranded hairpin RNAs of the target gene. The four transgenes were specifically targeted to positions 2046–2064 (A), 2031–2049 (B), 2048–2066 (C) and 1416–1434 bp (D) in the *MTf* gene (Genbank accession no.: NM_005929). They showed no homology to other human genes as shown using the BLAST program (http://www.ncbi.nlm.nih.gov/blast). As a control, we cloned a scrambled, non-specific transgene into the vector (pS-scrambled) (Ambion).

Human SK-Mel-28 melanoma cells were obtained from the American Type Culture Collection (MD) and cultured as described previously (7). Transfections of pS-MTf transgenes or pS-scrambled vectors were performed with Lipofectamine 2000 reagent (Invitrogen) and cells were selected and maintained in 1000 μg/ml of G418 (Invitrogen).

RT–PCR and western analysis

RNA was isolated using the TRIzol reagent as described above and RT–PCR analyses of transcripts were carried out by standard procedures (32) using the primers in Table I. Briefly, 0.3–1.0 μg of RNA was incubated with gene-specific oligonucleotides (0.2 μM final primer concentration) in a 50 μl volume containing 25 μl of 2× Reaction Mix (1.6 mM MgSO$_4$ and 200 μM dNTP) and 2 μl of SuperScript III RT/Platinum *Taq* Mix for 30 min at 50°C. After reverse transcription the samples were initially denatured for 3 min at 94°C. The reactions were then amplified for 20–35 PCR cycles that included a 90°C denaturation step for 30 s, 55–60°C annealing step for 30–60 s, a 68°C extension step for 60 s, with a final extension time of 5 min. As an

Table I. Primers for amplification of mouse and human mRNA

Pair no.	Primer name	Genotype/accession no.	Oligonucleotides (5′–3′)				Product size (bp)
			Forward	Priming sites	Reverse	Priming sites	
1	*mMTf*	NM_013900	AGGCTCCTGAGCGTGACTT	121–139	CACTGTGCTGTGCTTCAGG	795–813	693
2	*hMTf*	NM_005929	TCATCGCGGCCCAGGAGGCTG	266–286	GGCAGCCGGTTGGGGTCACAG	1137–1157	892
3	*mTfR1*	NM_011638	TCCCGAGGGTTATGTGGC	700–717	GGCGGAAACTGAGTATGATTGA	1002–1023	324
4	*hTfR1*	NM_003234	TCAGGTCAAAGACAGCGCTCA	833–853	TTGGGAATATGGAAGGAGACT	1300–1320	488
5	*mβ-actin*	NM_007393	CCCGCCACCAGTTCGCCATGG	64–84	AAGGTCTCAAACATGATCTGGGTC	437–460	397
6	*hβ-actin*	NM_001101	CCCGCCGCCAGCTCACCATGG	57–77	AAGGTCTCAAACATGATCTGGGTC	433–453	397
7	*hOAS1*	NM_016816	AGGTGGTAAAGGGTGGCTCC	203–222	ACAACCAGGTCAGCGTCAGAT	252–272	70
8	*mMef2a*	NM_001033713	GCCCTGATGCTGACGATT	629–646	TTCCGACTGTTCATTCCAAG	1120–1139	511
9	*hMEF2A*	NM_005587	TCTAGACATTGAGTCTCACTCTACCC	52–77	TTCTACAAGATCTGAGGTCCAGAG	260–283	232
10	*mGls*	XM_129846	GGCTAATGGTGGTTTCTG	1557–1574	TTCAACATGACCCTCTGC	2038–2055	499
11	*hGLS*	NM_014905	GGCTAATGGTGGTTTCTG	1532–1552	TTCTTATGGACGGTTTGA	2201–2221	690
12	*mTcf4*	NM_013685	GGGGCTCATACTCATCTT	843–860	GCCTGTCCTCCATTTCTA	1612–1629	787
13	*hTCF4*	NM_003199	GGCGGTTTGTGTGATTTTG	176–194	ATAGTTCCTGGACGGGCTTG	393–412	237
14	*mApod*	NM_007470	TTCTTTGCTTTGCGTTCC	747–764	CGGTGGTCAGGGATTCTA	1524–1541	795

internal control, β-actin was amplified from the same samples. Identities of transcripts were confirmed by DNA sequencing (8).

Protein isolation and western analysis were performed using established techniques, as described previously (33).

Labeling of Tf with Fe

Established techniques were used to label apo-Tf (Sigma Aldrich, MO) or apo-MTf (from Malcolm Kennard, Synapse Technologies, British Columbia, Canada) with ^{56}Fe or ^{59}Fe (Perkin-Elmer, Boston, MA) (19).

Iron uptake assay

Standard techniques in our laboratory were used to determine cellular ^{59}Fe uptake from ^{59}Fe–Tf (34,35). Briefly, cells were incubated with ^{59}Fe–Tf ([Tf] = 0.75 μM; [Fe] = 1.5 μM) for up to 240 min at 37°C. The culture plates were then placed on a tray of ice and the monolayer was washed four times with ice-cold PBS. The cells were subsequently incubated with the general protease, Pronase (1 mg/ml; Sigma), for 30 min at 4°C. The cells were removed from the plates using a plastic spatula and centrifuged at 14 000 r.p.m. for 1 min. This procedure resulted in the separation of Pronase-insensitive (internalized) ^{59}Fe in the cell pellet, while the Pronase-sensitive (membrane-bound) ^{59}Fe remained in the supernatant. Previous studies have demonstrated that this latter technique is valid for measuring internalized and membrane-bound ^{59}Fe–Tf uptake by cells (14,34). The supernatant and pellet were separated and placed in separate counting tubes. Radioactivity was measured on a γ-scintillation counter (Wallac, Compugamma, Finland).

In vitro cell proliferation and migration assays

Cell counts were performed using Trypan blue staining. DNA synthesis was measured via incorporation of ^{3}H-thymidine (Perkin-Elmer, MA) using standard procedures (36). Cell migration assays were performed over 18 h using Transwell filters in 24-well plates (Corning, NY) pre-coated with 0.15% gelatin (28). As a second measurement of cell migration and proliferation, wound scrape assays were also implemented (37,38).

Tumor biology in nude mice

Male nude mice (BALB/c-nu) were subcutaneously injected at one site on the right flank with 1×10^6 SK-Mel-28 cells, MTf/B1 or scrambled control cells. Tumor growth was measured by standard procedures (39).

Statistical analysis

Excluding the statistical analysis of the microarray results described above, all data were compared using Student's *t*-test. Results were expressed as mean ± standard error of the mean (SEM) or mean ± standard deviation (SD). Data were considered statistically significant when *P* < 0.05.

Results

Phenotypic characterization of *MTf*$^{-/-}$ mice

Melanotransferrin knockout mice of a mixed 129/SvJ and C57BL/6 background were generated by homologous recombination in ES cells, as described previously (9). In this procedure, exon 1 was cloned in the reverse orientation, while exons 2, 3 and 4 that encode the Fe-binding domain (40) and the intervening introns of the *MTf* gene were removed. This targeting strategy disrupted the promoter region, the translation initiation codon and the Fe-binding domain and resulted in no *MTf* mRNA or protein product (9).

The *MTf*$^{-/-}$ mice displayed no differences in reproduction, growth, development or histology compared with *MTf*$^{+/+}$ littermates. Offspring from *MTf*$^{+/-}$ matings had a distribution of 26% *MTf*$^{+/+}$, 48% *MTf*$^{+/-}$ and 26% *MTf*$^{-/-}$ (*n* = 312). This was consistent with a normal Mendelian inheritance ratio of 25% wild-types, 50% heterozygotes and 25% homozygotes. Litter sizes of *MTf*$^{+/+}$ matings were comparable with the average litter sizes of *MTf*$^{-/-}$ matings. There were no significant differences in mouse body weight from 3 to 15 weeks of age (Figure 1A and B). For example, at 12 weeks of age, the weights of male *MTf*$^{+/+}$ mice (26.5 ± 0.4 g; mean ± SEM, *n* = 22) were not significantly different to male *MTf*$^{-/-}$ littermates (27.5 ± 0.6 g, *n* = 27) (Figure 1A). Similarly, the weights of female *MTf*$^{+/+}$ mice (21.2 ± 0.4 g,

n = 14) were not significantly different to female *MTf*$^{-/-}$ littermates (20.4 ± 0.5 g, *n* = 18) (Figure 1B). Behavioral assessment using intruder and open-field studies (41–43) showed no significant difference between the *MTf*$^{+/+}$ and *MTf*$^{-/-}$ genotypes (data not shown).

Examination of organ-to-total body weight ratios at autopsy indicated no gross changes between genotypes (Figure 1C and D), or histological differences in the tissues (data not shown). To address the suggestion that MTf may play a role in brain Fe transport (21,22,44), we assessed brain Fe levels in mice maintained for 4 weeks on either a basal (0.02%) Fe or high (2.00%) Fe diet (Figure 1E and F). Regardless of diet, no significant differences were observed in either male or female *MTf*$^{-/-}$ mice compared with *MTf*$^{+/+}$ littermates. The effect of dietary Fe challenge on Fe levels in the liver, spleen, heart and kidney was reported in our previous study, where no differences were observed between the genotypes (9).

A panel of hematological indices (Table II) and selected serum biochemistry parameters (Table III) were assessed with no significant differences being detected between *MTf*$^{-/-}$ and *MTf*$^{+/+}$ littermates except in alkaline phosphatase (ALP) levels in male animals. However, this significant (*P* < 0.05) decrease in ALP levels was within the normal range (45). Moreover, this difference in ALP levels was not observed when comparing female *MTf*$^{-/-}$ and *MTf*$^{+/+}$ mice. All the hematological and biochemical parameters assessed were within physiological limits observed in mice (45,46). A broader serum biochemistry and hematological screen, which included amylase, creatine kinase-MB, cholesterol, glucose, triglycerides, urea, $Ca^{+2}/Mg^{+2}/PO_4^{-3}$, prothrombin and partial prothrombin time and differential cell counts (including neutrophils, basophils and eosinophils) also showed no significant differences between *MTf*$^{-/-}$ and *MTf*$^{+/+}$ littermates (data not shown).

Male and female mice were assessed as separate groups owing to the known differences in Fe metabolism between the two sexes (47,48). All of the above-mentioned parameters were also assessed as part of a longevity study when mice were 18 months old, with no significant differences being observed (data not shown).

MTf expression is not essential for normal Fe metabolism

MTf is a Tf homolog and shares many of its characteristics, including the ability to bind Fe (3,40). To determine whether MTf has a role in Fe metabolism, serum and tissue Fe indices were measured in 12-week-old *MTf*$^{-/-}$ and *MTf*$^{+/+}$ littermates. In male or female mice, serum Fe levels, Tf saturation, TIBC and tissue Fe levels were not significantly different (*P* > 0.05) in *MTf*$^{-/-}$ animals compared with *MTf*$^{+/+}$ littermates (Tables IV and V).

Since MTf has an Fe-binding site identical to Tf (1,3,11,13), it could bind other vital metals such as Cu^{2+} and Zn^{2+} (49). Hence, it was important to examine the effects of the *MTf* null allele on tissue Cu and Zn levels. As found for Fe, no differences were observed comparing *MTf*$^{-/-}$ animals with their *MTf*$^{+/+}$ littermates (data not shown).

Comparative data analysis of the differential gene expression between MTf$^{+/+}$ and MTf$^{-/-}$ mice

Considering that there were no observable phenotypic differences between the *MTf*$^{-/-}$ and *MTf*$^{+/+}$ littermates, we embarked upon microarray analysis to determine if there
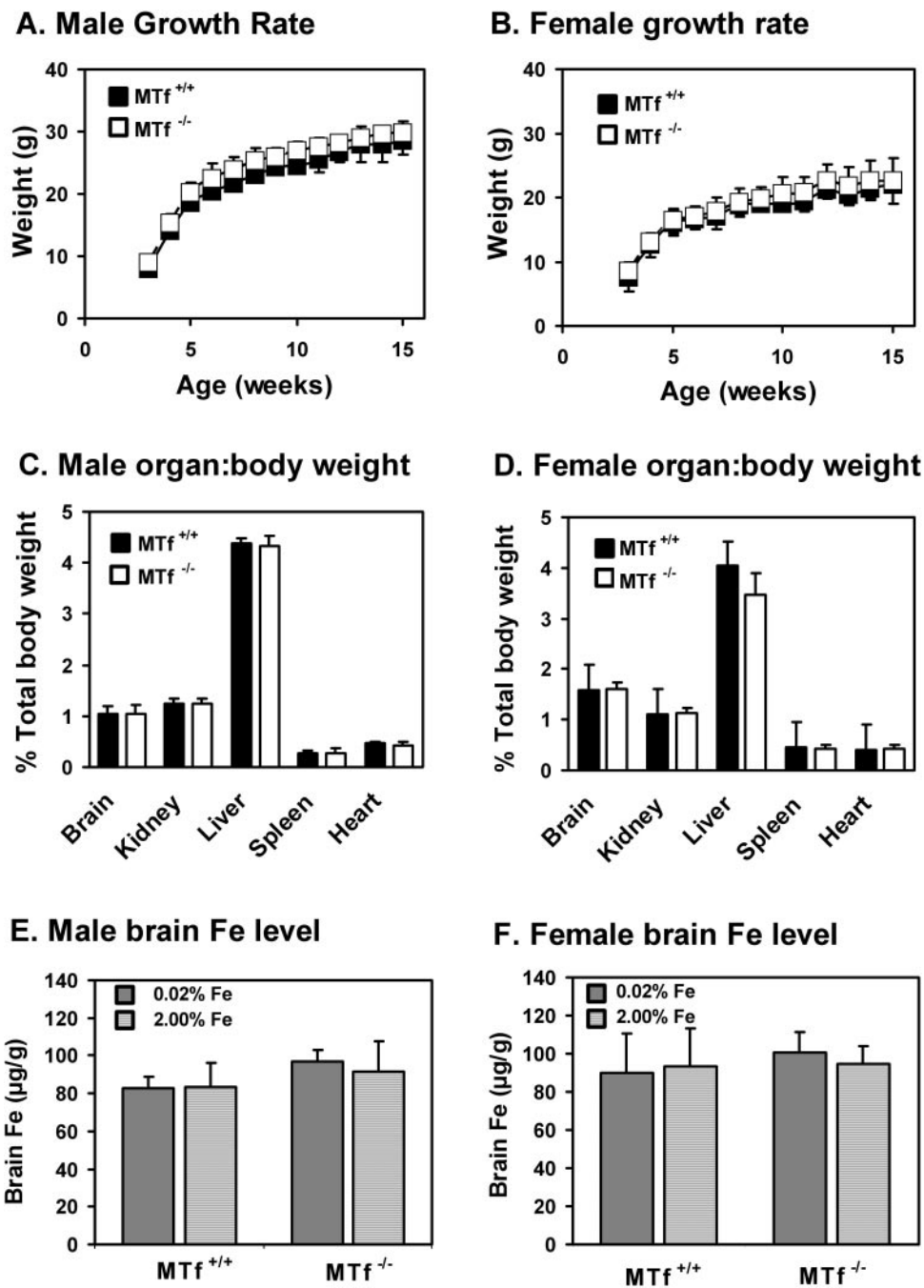
Fig. 1. Examination of growth rates, organ-to-body weight ratios and brain Fe levels of $MTf^{-/-}$ compared with $MTf^{+/+}$ littermates. Mice were maintained on a basal rodent chow diet, watered *ad libitum* and routinely weighed each week. Over 15 weeks there were no significant differences in total body weight or growth rates between either male (**A**) or female (**B**) $MTf^{-/-}$ and $MTf^{+/+}$ littermates ($n = 14$–27). The organ-to-total body weight ratios at autopsy of the brain, kidney, liver, spleen and heart were examined in male (**C**) and female (**D**) $MTf^{-/-}$ and $MTf^{+/+}$ littermates ($n = 5$). No differences were observed in the ratios. (A–D) Results are expressed as mean ± SD. To examine brain Fe levels, mice were maintained on either basal rodent chow (0.02% Fe) or high Fe chow (2.00%) for 4 weeks. The levels of Fe in the brain were then determined by ICP-AES. There were no significant differences in brain Fe levels in $MTf^{-/-}$ mice maintained on a basal or high Fe diet compared with $MTf^{+/+}$ littermates in both males (**E**) and females (**F**). Results (E and F) are expressed as mean ± SD ($n = 6$).

were changes in gene expression that may lead to a further understanding of MTf function. The levels of gene expression were determined from brain tissue RNA samples that were hybridized to the Mouse Genome 430 2.0 array GeneChip (Affymetrix). Mouse brain had the highest MTf expression in both sexes (8) and was used to determine differential gene expression between $MTf^{-/-}$ and $MTf^{+/+}$ mice.

The top 30 genes showing both the largest positive and negative fold changes are summarized in Figure 2A. A positive value of the log$_2$-fold change in expression indicates upregulation in $MTf^{-/-}$ samples relative to the wild-type animals, while a negative value indicates downregulation. Analysis of the genes affected by ablation of MTf (Figure 2A–C) using NetAffx software (http://www.affymetrix.com/analysis/index.affx)

Table II. Hematological indices in $MTf^{-/-}$ mice compared with their $MTf^{+/+}$ littermates at 12 weeks of age

Sex	N	Genotype	RBC (10^{12}/l)	HGB (g/l)	HCT	MCV (fl)	WBC (10^9/l)
M	19	$MTf^{+/+}$	8.6 ± 0.2	134 ± 3	0.45 ± 0.01	52.2 ± 0.5	6.8 ± 0.7
	21	$MTf^{-/-}$	9.0 ± 0.1	138 ± 2	0.47 ± 0.01	52.1 ± 0.4	6.3 ± 0.5
F	17	$MTf^{+/+}$	9.2 ± 0.1	146 ± 4	0.48 ± 0.01	52.5 ± 0.4	5.6 ± 0.4
	25	$MTf^{-/-}$	9.1 ± 0.1	132 ± 2	0.47 ± 0.01	51.9 ± 0.4	5.5 ± 0.3

Values expressed as mean ± SEM.
M, male; F, female; HCT, hematocrit; HGB, hemoglobin; MCV, mean corpuscular volume; RBC, red blood cells; WBC, white blood cells.

Table III. Selected serum chemistry indices in $MTf^{-/-}$ mice compared with their $MTf^{+/+}$ littermates at 12 weeks of age

Sex	n	Genotype	Creatinine (μmol/l)	Protein (g/l)	AST (U/l)	ALP (U/l)	ALT (U/l)
M	12	$MTf^{+/+}$	44 ± 1	46 ± 1	108 ± 13	121 ± 6*	43 ± 5
	16	$MTf^{-/-}$	43 ± 2	44 ± 1	125 ± 10	98 ± 5*	51 ± 7
F	7	$MTf^{+/+}$	42 ± 1	48 ± 1	111 ± 11	150 ± 6	33 ± 3
	6	$MTf^{-/-}$	44 ± 2	45 ± 1	121 ± 6	139 ± 11	45 ± 4

Values expressed as mean ± SEM.
M, male; F, female; ALP, alkaline phosphatase; ALT, alanine aminotransferase; AST, aspartate aminotransferase.
*$P < 0.05$ as determined by Student's t-test.

Table IV. Serum Fe indices in $MTf^{-/-}$ mice compared with their $MTf^{+/+}$ littermates at 12 weeks of age

Sex	n	Genotype	Serum Fe (μmol/l)	TIBC (μmol/l)	Tf saturation (%)
M	16	$MTf^{+/+}$	57.5 ± 2.5	105.2 ± 3.8	73 ± 3
	21	$MTf^{-/-}$	50.7 ± 2.7	96.0 ± 4.2	67 ± 3
F	13	$MTf^{+/+}$	65.2 ± 6.5	115.7 ± 8.1	81 ± 6
	9	$MTf^{-/-}$	55.3 ± 4.8	113.4 ± 9.9	80 ± 7

Values expressed as mean ± SEM.
M, male; F, female; TIBC, total iron-binding capacity.

Table V. Tissue Fe stores in $MTf^{-/-}$ mice compared with their $MTf^{+/+}$ littermates at 12 weeks of age

Sex	n	Genotype	Tissue Fe level (μg/g) (mean ± SEM)				
			Liver	Spleen	Brain	Heart	Kidney
Male	25	$MTf^{+/+}$	276 ± 14	3241 ± 186	69 ± 4	643 ± 32	259 ± 11
	26	$MTf^{-/-}$	291 ± 17	2864 ± 166	66 ± 4	588 ± 32	243 ± 12
Female	15	$MTf^{+/+}$	368 ± 17	4858 ± 396	69 ± 4	573 ± 31	331 ± 22
	17	$MTf^{-/-}$	426 ± 20	4202 ± 392	67 ± 3	534 ± 28	309 ± 22

indicated that they have roles in gene transcription, differentiation and development, regulation of cellular metabolism, transport and cell adhesion.

Similar to the mRNA and protein data from the $MTf^{-/-}$ animal studies (9), microarray analysis demonstrated no differential expression of *TfR1* or any other molecules known to be involved in Fe metabolism between $MTf^{-/-}$ and $MTf^{+/+}$ mice. These data relating to *TfR1* expression again confirm our previous observations that deletion of *MTf* did not affect the Fe pools that regulate *TfR1* expression (9). In addition, and as expected, gene array assessment of *MTf* expression showed that it was downregulated in the $MTf^{-/-}$ mice compared with their $MTf^{+/+}$ littermates.

To validate the expression of the 30 genes showing the largest changes in the array data (Figure 2A), RT–PCR was used. Increased expression of the following genes was observed in $MTf^{-/-}$ mice when compared with their $MTf^{+/+}$ littermates: *Mef2a, Gls* and *Tcf4* (Figure 2B). Conversely, expression of the *Apod* and *MTf* genes were downregulated in $MTf^{-/-}$ mice compared with $MTf^{+/+}$ littermates (Figure 2B). Densitometric analysis of the RT–PCR data was used to quantify the magnitude of change in gene expression. Expression of *Mef2a* mRNA was found to be 4-fold higher (log$_2$ ratios of +2.03) in $MTf^{-/-}$ mice compared with $MTf^{+/+}$ littermates, while *Gls* and *Tcf4* mRNA expression were increased by 2-fold (log$_2$ ratios of +1.03) and 3-fold (log$_2$ ratios of +1.63), respectively (Figure 2C). Examination of *Apod* mRNA expression indicated a 5-fold downregulation (log$_2$ ratios of −2.39) (Figure 2C) in $MTf^{-/-}$ mice compared with $MTf^{+/+}$ littermates. In addition to the samples submitted
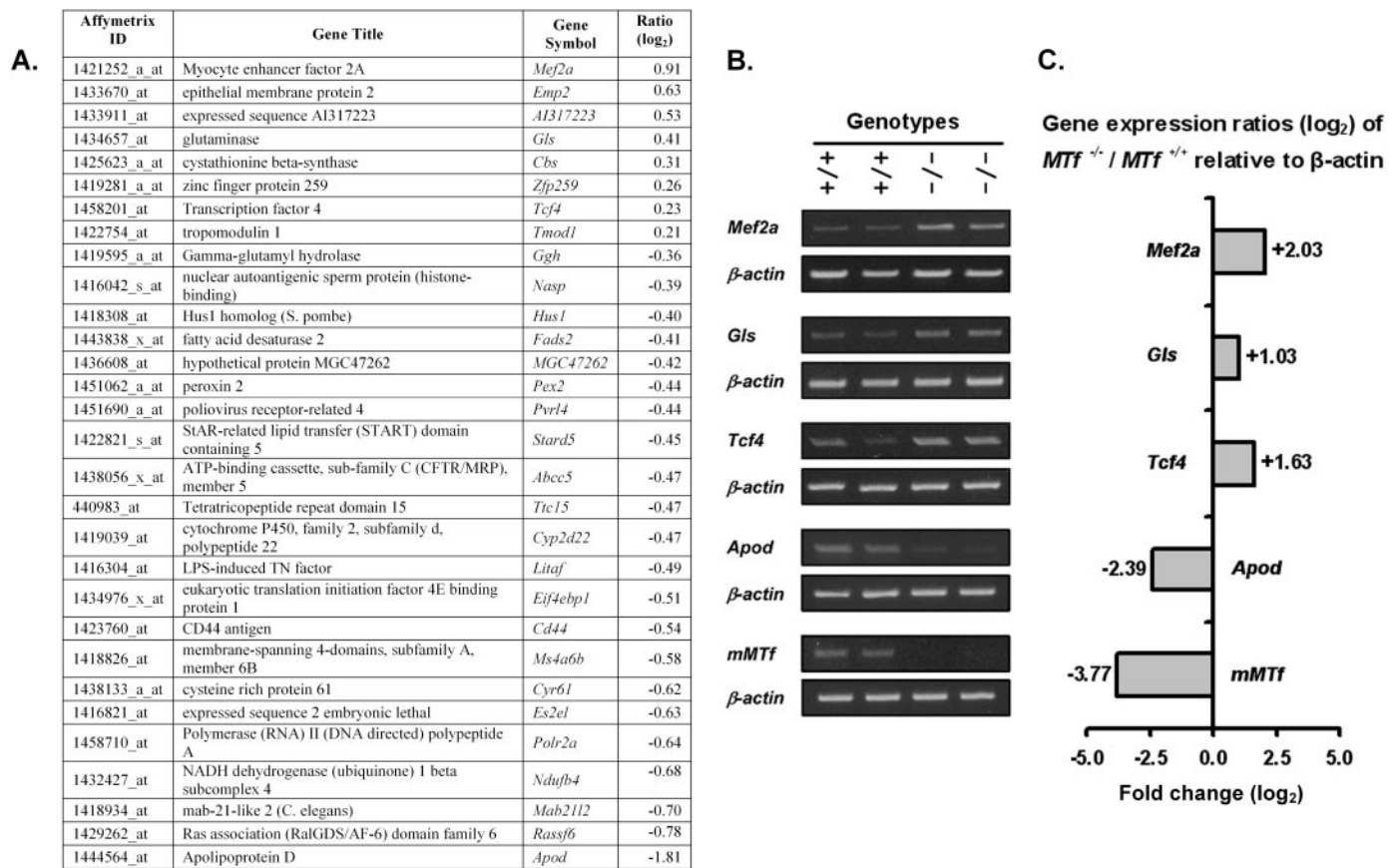
2161

A.

Affymetrix ID	Gene Title	Gene Symbol	Ratio (log₂)
1421252_a_at	Myocyte enhancer factor 2A	*Mef2a*	0.91
1433670_at	epithelial membrane protein 2	*Emp2*	0.63
1433911_at	expressed sequence AI317223	*AI317223*	0.53
1434657_at	glutaminase	*Gls*	0.41
1425623_a_at	cystathionine beta-synthase	*Cbs*	0.31
1419281_a_at	zinc finger protein 259	*Zfp259*	0.26
1458201_at	Transcription factor 4	*Tcf4*	0.23
1422754_at	tropomodulin 1	*Tmod1*	0.21
1419595_a_at	Gamma-glutamyl hydrolase	*Ggh*	-0.36
1416042_s_at	nuclear autoantigenic sperm protein (histone-binding)	*Nasp*	-0.39
1418308_at	Hus1 homolog (S. pombe)	*Hus1*	-0.40
1443838_x_at	fatty acid desaturase 2	*Fads2*	-0.41
1436608_at	hypothetical protein MGC47262	*MGC47262*	-0.42
1451062_a_at	peroxin 2	*Pex2*	-0.44
1451690_a_at	poliovirus receptor-related 4	*Pvrl4*	-0.44
1422821_s_at	StAR-related lipid transfer (START) domain containing 5	*Stard5*	-0.45
1438056_x_at	ATP-binding cassette, sub-family C (CFTR/MRP), member 5	*Abcc5*	-0.47
440983_at	Tetratricopeptide repeat domain 15	*Ttc15*	-0.47
1419039_at	cytochrome P450, family 2, subfamily d, polypeptide 22	*Cyp2d22*	-0.47
1416304_at	LPS-induced TN factor	*Litaf*	-0.49
1434976_x_at	eukaryotic translation initiation factor 4E binding protein 1	*Eif4ebp1*	-0.51
1423760_at	CD44 antigen	*Cd44*	-0.54
1418826_at	membrane-spanning 4-domains, subfamily A, member 6B	*Ms4a6b*	-0.58
1438133_a_at	cysteine rich protein 61	*Cyr61*	-0.62
1416821_at	expressed sequence 2 embryonic lethal	*Es2el*	-0.63
1458710_at	Polymerase (RNA) II (DNA directed) polypeptide A	*Polr2a*	-0.64
1432427_at	NADH dehydrogenase (ubiquinone) 1 beta subcomplex 4	*Ndufb4*	-0.68
1418934_at	mab-21-like 2 (C. elegans)	*Mab21l2*	-0.70
1429262_at	Ras association (RalGDS/AF-6) domain family 6	*Rassf6*	-0.78
1444564_at	Apolipoprotein D	*Apod*	-1.81

Fig. 2. Comparative data analysis and RT–PCR of genes showing differential expression between *MTf*⁻/⁻ and *MTf*⁺/⁺ mice. RNA from *MTf*⁻/⁻ and *MTf*⁺/⁺ littermates was subjected to gene array analysis using the Affymetrix Mouse Genome 430 2.0 array GeneChips (*see* Materials and methods). (**A**) The list of 30 genes showing the most significant differential expression between genotypes. (**B**) RT–PCR of some of the genes assessed by their log₂ value to show differential expression from the microarray data. (**C**) Densitometric analysis of RT–PCR. The bar graph represents the change in expression of genes affected as a result of MTf ablation. Results in (B) and (C) were performed on both RNA samples sent for gene array and independent samples from other mice. The results are representative of at least three separate experiments performed.

for gene array analysis, we also confirmed the data independently on RNA samples from other *MTf*⁻/⁻ and *MTf*⁺/⁺ mice.

Downregulation of MTf expression in SK-Mel-28 cells by PTGS

While there were some differential gene expression in the microarray study, no observable phenotype was detected in the *MTf*⁻/⁻ mice compared with *MTf*⁺/⁺ littermates. Indeed, the role of MTf may only become apparent in melanoma cells where it is expressed at very high levels (1,2). To assess this, we stably transfected SK-Mel-28 cells with a pS-MTf vector, which encoded each of the four transgenes that transcribe a 19mer anti-MTf hairpin siRNA. As a control, SK-Mel-28 cells were transfected with the same vector containing a scrambled, non-specific sequence. Of the four siRNAs specifically targeted to the human *MTf* gene, we found that the vector containing the B transgene (pS-MTf/B1) consistently gave us the most pronounced downregulation of MTf expression and inhibition of cellular proliferation. The other three transgenes resulted in less MTf downregulation and not as marked reduction in proliferation (data not shown). Therefore, all further experiments used clones from the B transgene. The fact that all transgenes reduced MTf expression to some degree suggested that the effect observed was not due to possible off-target effects of the siRNA. The clones obtained from transfection with the pS-MTf/B1 vector

demonstrated downregulation of *MTf* mRNA and protein by >90 (Figure 3A) and >80% (Figure 3B), respectively, compared with cells transfected with the scrambled transgene. In Figure 3B, two MTf protein bands were visible on the western blot at 79- and 82-kDa, which are the result of post-translational modification of MTf (50).

Multiple transfection experiments with the pS-MTf/B1 vector 6 months after the initial study showed similar downregulation of MTf expression in SK-Mel-28 cells, indicating that this was not a clonal effect. Cells transfected with a scrambled, non-specific transgene displayed no reduction in *hMTf* mRNA or protein expression compared with non-transfected SK-Mel-28 parent cells (data not shown). To exclude the possibility that siRNA was eliciting an interferon-stimulated response that could affect cellular phenotypes, we performed RT–PCR to assess the expression of the interferon-target gene, *2′,5′-oligoadenylate synthetase 1* (*hOAS1*) (51). There were no differences in *hOAS1* expression between the scrambled control cell line, MTf/B1 (Figure 3A), and SK-Mel-28 cells (data not shown). As another control, the effect of downregulation of MTf on the expression of the Fe-regulated gene, *hTfR1* (52), was assessed. There was no alteration in *hTfR1* mRNA expression in the MTf/B1 cell line compared with the scrambled control (Figure 3A). The expression of the transcription factors, *hMEF2A* and *hTCF4*, were assessed in MTf/B1 and scrambled
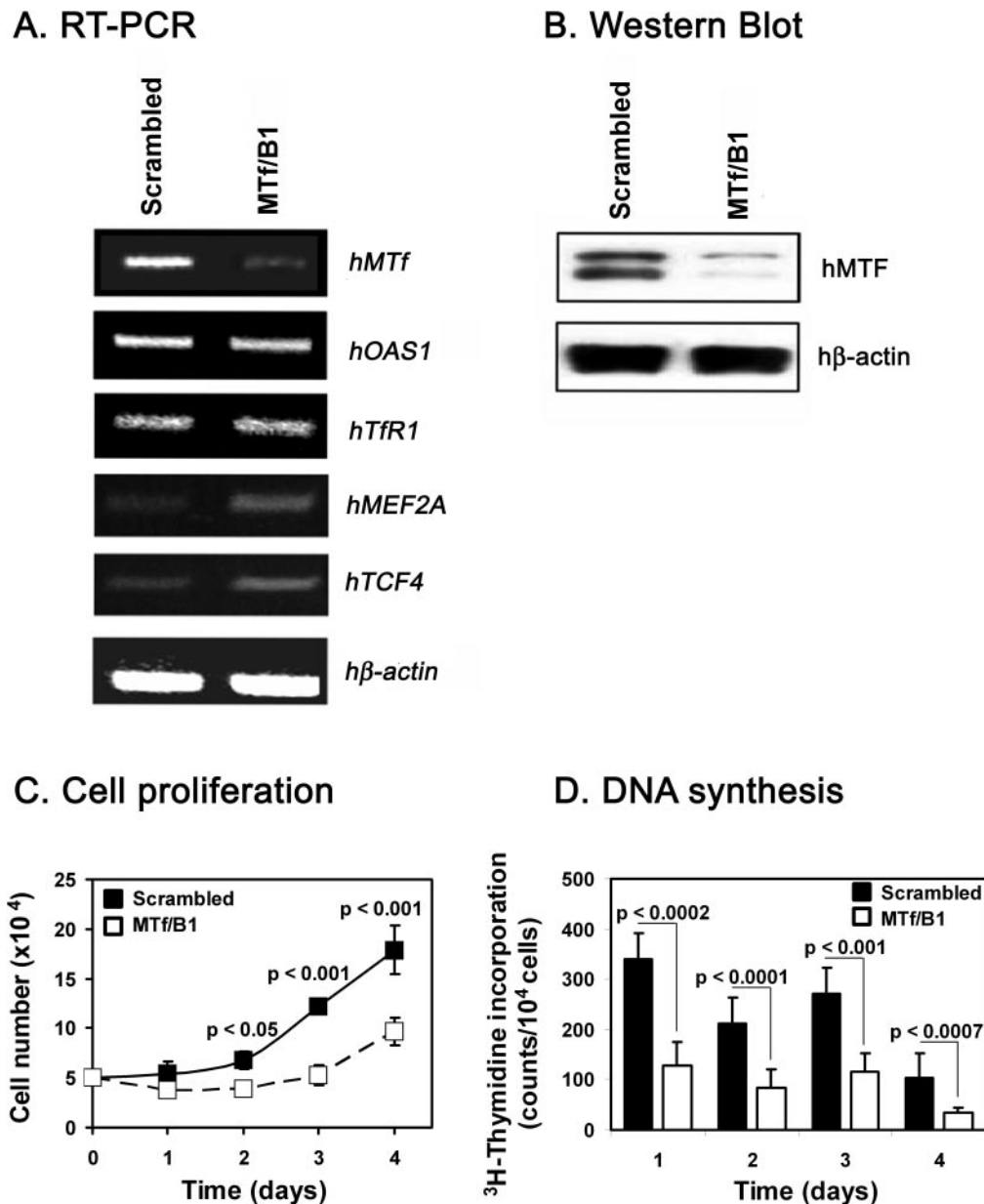
A. RT-PCR

B. Western Blot

C. Cell proliferation

D. DNA synthesis

Fig. 3. PTGS of MTf in melanoma cells leads to decreased *MTf* mRNA and protein levels and a decrease in cellular proliferation and DNA synthesis. SK-Mel-28 melanoma cells were stably transfected with a vector that contained a cloned transgene that encodes a short 19mer double-stranded hairpin RNA to target *MTf* mRNA. As a control, a second vector containing a non-specific (scrambled) hairpin siRNA was similarly transfected into cells. Clones were selected in G418 and are referred to as 'MTf/B1' and 'scrambled control'. (**A**) RT–PCR analysis demonstrates marked downregulation of *hMTf* mRNA in the MTf/B1 cell line compared with scrambled control cells. The expression of *hTfR1* and *hOAS1* remain unchanged. The transcription factors *hMEF2A* and *hTCF4* were upregulated in MTf/B1 cells. (**B**) Western blot analysis demonstrated a >80% decrease in MTf protein expression in the MTf/B1 cell line compared with scrambled control cells. (**C**) Cellular proliferation was assessed by viable cell counts using Trypan blue. MTf/B1 cells showed depressed growth when compared with cells transfected with the scrambled transgene. (**D**) ^{3}H-thymidine incorporation was significantly decreased in the MTf/B1 cell line on Days 1–4 compared with cells transfected with the scrambled control vector. Results in (A) and (B) are representative results in a typical experiment from three separate experiments performed, while (C) and (D) are presented as mean ± SD (six determinations) in a typical experiment from at least three separate experiments performed.

control cells. As found for the $MTf^{-/-}$ mice, these transcription factors were upregulated in the MTf/B1 cell line (Figure 3A). However, there was no significant change in *hAPOD* expression, while *hGLS* was not detected (data not shown).

During culture of MTf/B1 cells it became apparent that their growth was slower than cells transfected with the scrambled, non-specific transgene. To quantify this, proliferation was assessed using viable cell counts with Trypan blue staining. Over 4 days, MTf/B1 cells showed decreased growth when compared with cells transfected with the scrambled transgene (Figure 3C), and this was significant on Days 2 ($P < 0.05$), 3 and 4 ($P < 0.001$). In contrast, there was no growth inhibition in scrambled control cells when compared with the parent SK-Mel-28 cells (data not shown). DNA synthesis in MTf/B1 cells was also examined using ^{3}H-thymidine incorporation and was found to be significantly decreased ($P < 0.001$) on Days 1–4 compared with scrambled

control cells (Figure 3D). Fluorescent staining for cell viability (using acridine orange, propidium iodide and Hoechst 33258) indicated that the depressed proliferation was not due to apoptosis or necrosis (data not shown).

Addition of Fe, apo-MTf or holo-MTf does not rescue depressed proliferation in melanoma cells with decreased MTf expression

To further assess the hypothesis that MTf may potentially act as an Fe transport molecule to aid melanoma proliferation (3), we examined whether exogenous Fe could restore the depressed growth of MTf/B1 cells. To do this, cells were incubated with ferric ammonium citrate (FAC; 100 µg/ml), which is well known to effectively donate Fe to cells (34,53). Previously, we showed that FAC donates Fe to the same cell type used here (SK-Mel-28 cells) and downregulates both *hTfR1* mRNA and protein levels (7,34). These studies with FAC resulted in no restoration or increase of proliferation in

MTf/B1 cells or cells transfected with the scrambled siRNA transgene (Figure 4A). As a positive control for the ability of FAC to donate Fe to cells, *hTfR1* mRNA expression was assessed and shown to be markedly decreased after an incubation of 1–4 days with this Fe source (data not shown). The lack of effect of FAC on proliferation suggested that the cells were Fe-replete probably because they were grown under optimal conditions in media containing 10% FCS. The inability of FAC to rescue the slower growth of MTf/B1 cells suggested that its depressed proliferation was not due to Fe deprivation because of decreased MTf expression.

As a measure of Fe status in cells cultured under standard growth conditions, *hTfR1* mRNA expression was assessed and found not to be increased in the MTf/B1 cell line compared with cells transfected with the scrambled control vector (Figure 3A). These results showed that the MTf/B1 cells with low MTf expression were not Fe-deprived compared with the scrambled control. When holo-Tf
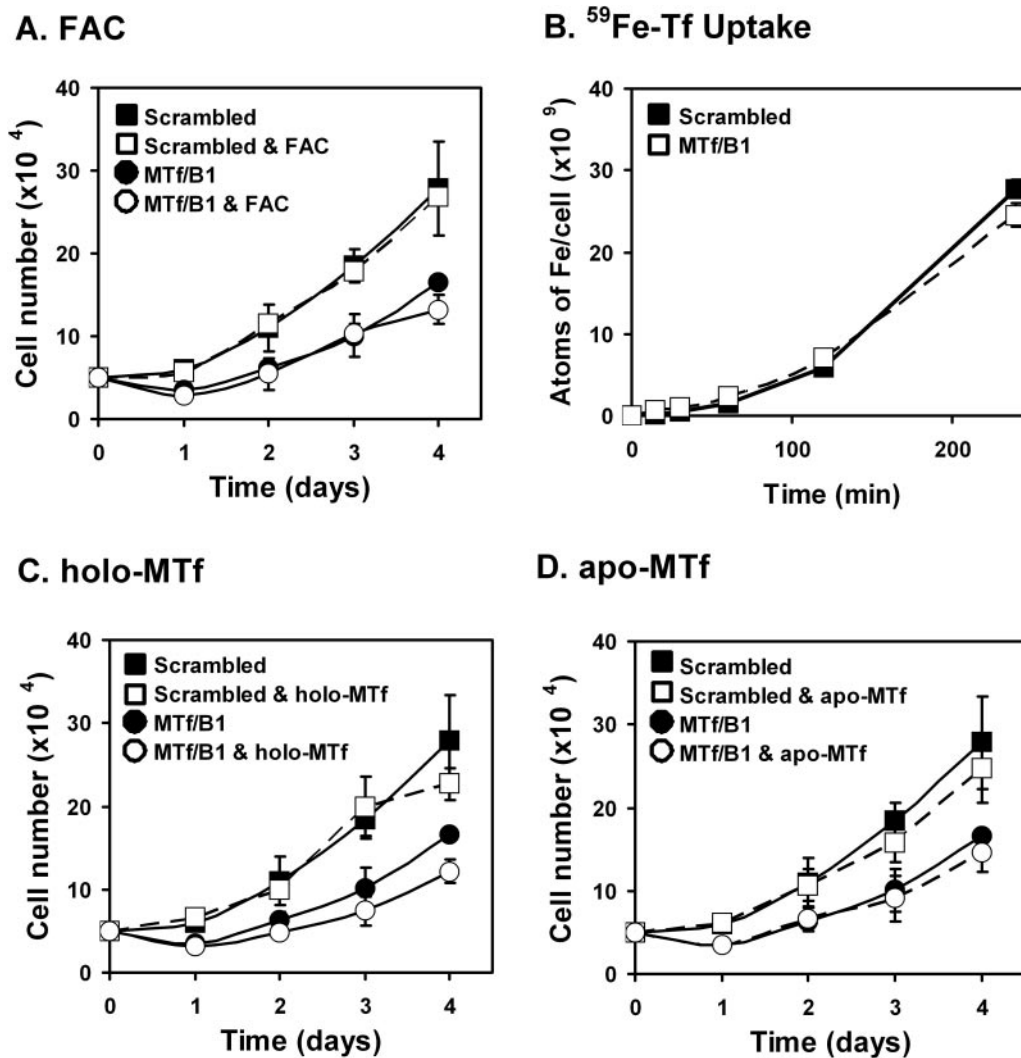
Fig. 4. Addition of Fe, soluble apo-MTf or soluble holo-MTf does not rescue decreased melanoma cell proliferation induced by MTf downregulation. SK-Mel-28 melanoma cells were stably transfected with control vector expressing scrambled non-specific control siRNA or the anti-MTf siRNA transgene to generate MTf/B1 and scrambled cells, respectively. (**A**) Proliferation rates were measured using viable cell counts after addition of Fe as FAC (100 µg/ml). Exogenous Fe did not restore proliferation in cells showing downregulation of MTf. (**B**) There was no significant difference in ^{59}Fe uptake from ^{59}Fe–Tf (0.75 µM) as a function of time between the scrambled control cell line and the MTf/B1 cell type with low MTf expression. (**C**) Addition of holo-MTf (1.0 µM) or (**D**) apo-MTf (1.0 µM) did not rescue the depressed proliferation rate of the MTf/B1 cell line compared with the scrambled control. Results are mean ± SD (three determinations) in a typical experiment from three separate experiments performed.

([Fe] = 1.5 μM) was added as an Fe donor, it also did not stimulate growth (data not shown), again probably because these cells were Fe-replete.

To further examine the relationship between MTf function and Fe metabolism, we performed ^{59}Fe uptake assays using ^{59}Fe–Tf (0.75 μM). These studies showed no significant difference in ^{59}Fe uptake from ^{59}Fe–Tf between MTf/B1 cells and the scrambled control (Figure 4B), suggesting that MTf had a negligible role in Fe uptake from Tf. The fact that ^{59}Fe–Tf uptake was not greater than the scrambled control agrees with our data indicating no difference in *hTfR1* mRNA expression between MTf/B1 cells and the scrambled control (Figure 3A). These results support the finding that MTf/B1 cells were not Fe-deplete owing to low MTf expression.

A previous study suggested that sMTf can inhibit SK-Mel-28 cellular migration and that the balance between the soluble and membrane-bound forms of MTf can regulate this process (28). Hence, it was important to determine if incubating these cells with sMTf could restore proliferation of MTf/B1 cells. However, addition of holo-sMTf (Figure 4C) or apo-sMTf (Figure 4D) at a concentration well above those used in a previous study (1 μM) (17) had little effect on MTf/B1 cells or the scrambled control. This indicates that it is membrane-bound MTf that is important for proliferation.

Inhibition of MTf expression decreases cell migration

The suggestion that MTf may be involved in migration was assessed by examining the ability of melanoma cells to pass from the upper to the lower levels of a transwell filter (Figure 5A) and their ability to repair a 'wound' in a monolayer (Figure 5B). The MTf/B1 cell line showed a significant decrease ($P < 0.01$) in migration over 18 h compared with the scrambled control (Figure 5A). Since the cells do not significantly proliferate over 18 h (Figures 3C and 4A, C and D), the effect was unlikely to be due to a difference in growth rate. The ability of the cells to proliferate and migrate was also assessed via a wound closure assay (Figure 5B). This assay is an indirect measure of cell migration, as the effects of proliferation must also be taken into account. Scrambled control cells had closed the wound in the monolayer after 60 h, whereas MTf/B1 cells only begun to close the wound after 72 h (Figure 5B).

Inhibition of MTf expression by PTGS results in depressed tumor growth in nude mice

To examine the effect of decreased MTf expression on growth *in vivo*, the proliferation of MTf/B1 cells compared with SK-Mel-28 and scrambled control cells was assessed by subcutaneous injection into nude mice and the growth of the tumors was examined (Figure 5C). After 30 days, the tumor volume arising from the MTf/B1 clone was significantly ($P < 0.04$) smaller, namely 20 and 22% of that found for SK-Mel-28 or the scrambled control cells, respectively (Figure 5C). In addition, using the MTf/B1 cell type, tumors only developed in 4 out of 10 animals, while 9 out of 10 mice developed tumors when injected with SK-Mel-28 or the scrambled control cells. Examination of MTf protein levels in the harvested tumors after 30 days demonstrated that MTf expression in the MTf/B1 cell type was 20% of that of the parent cell or the scrambled control cells (Figure 5D). These results demonstrated that MTf expression remained depressed in the MTf/B1 cell line while *in vivo*.

Discussion

There is no conclusive evidence regarding the function of MTf, despite its suggested role in diverse metabolic processes including Fe metabolism and cellular differentiation (22,24,27,40,54). Since MTf possesses a functional Fe-binding site (3,13), a role in Fe metabolism appears plausible, particularly in malignant melanoma cells that express high levels of this tumor antigen (3). In the current study, two models using ablation and downregulation of MTf expression were developed to determine its function. First, a $MTf^{-/-}$ mouse model was generated by targeted disruption of the *MTf* gene to assess its function *in vivo*. Second, to examine the role of MTf in neoplastic cells, we downregulated MTf expression by PTGS using SK-Mel-28 melanoma cells, which express high MTf levels (10).

Our studies demonstrated that $MTf^{-/-}$ mice were viable, developed normally and showed no obvious morphological, histological, behavioral, hematological or Fe status changes when compared with $MTf^{+/+}$ littermates. In contrast to other studies indicating a role for MTf in brain Fe metabolism (16,21,22), no obvious changes were observed in brain Fe levels between $MTf^{-/-}$ and $MTf^{+/+}$ animals (Figure 1E and F). This supports the hypothesis that MTf had no essential role in normal Fe metabolism or Fe supply to the brain. In addition, other studies have not confirmed a role for MTf in brain Fe metabolism (55,56).

Interestingly, disruption of another Tf homolog, namely lactoferrin, also led to no phenotype (57), suggesting that these molecules do not play essential roles in Fe metabolism and may have other functions (40). In contrast, loss of function of molecules involved in Fe metabolism (58–63) has dramatic consequences. Indeed, in the case of TfR1, there are lethal effects *in utero* (59). Clearly, if MTf had an essential role in Fe homeostasis, significant alterations in Fe indices, if not a deleterious phenotype, would have been apparent.

The current investigation supports our previous *in vitro* studies using melanoma cells that demonstrated that membrane-bound MTf or sMTf did not play an important role in Fe uptake (7,15,18,19). These results were confirmed by others using different cell types (64). Furthermore, sMTf did not bind to TfR1 or TfR2 to donate Fe to cells (19,20). Other studies also suggest that MTf does not play a key role in Fe metabolism. For instance, unlike TfR1, which is upregulated to supply Fe for DNA synthesis in the S phase (65), MTf expression remained constant throughout the cell cycle (66). Moreover, in contrast to TfR1, MTf is not regulated by cellular Fe status (4,7) and is not upregulated in dividing cells (67). Collectively, these data and our previous results (9) demonstrate that MTf is not essential for normal Fe homeostasis.

As there was no obvious phenotype in the *MTf* knockout mouse, gene array analysis was employed to identify any changes in the gene expression profile of mice with the *MTf* null allele. These studies showed no changes in the expression of molecules known to be involved in Fe metabolism. However, the analysis did identify genes that were differentially expressed between $MTf^{-/-}$ and $MTf^{+/+}$ littermates. The products of these genes have roles in processes such as transcription, differentiation and development, regulation of cellular metabolism, transport and cell adhesion. Subsequent analysis of these changes using RT–PCR confirmed that the genes *Mef2a, Tcf4* and *Gls* were upregulated, while
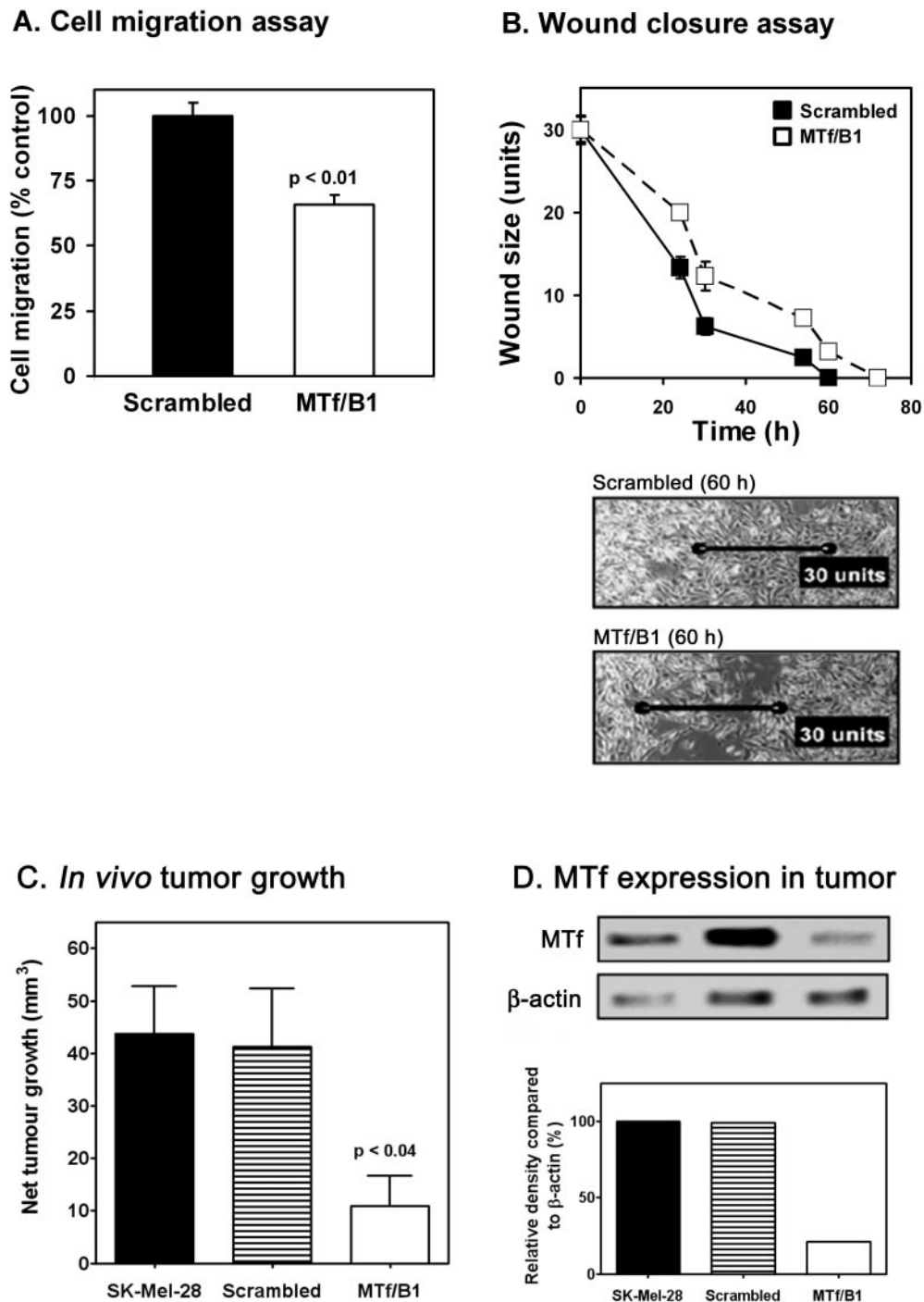
A. Cell migration assay

B. Wound closure assay

C. *In vivo* tumor growth

D. MTf expression in tumor

Fig. 5. Downregulation of MTf expression reduces SK-Mel-28 melanoma cell migration *in vitro* and decreases tumor growth *in vivo*. (**A**) Cell migration rates through a transwell chamber over 18 h by SK-Mel-28 melanoma cells stably transfected with anti-MTf siRNA (MTf/B1) or scrambled control siRNA. (**B**) MTf/B1 cells showed reduced proliferation and migration assessed by the 'wound' closure assay when compared with the scrambled control. Control cells closed the wound after 60 h, while MTf/B1 cells begin to close the wound after 72 h. The photograph shows a wound in the scrambled and MTf/B1 monolayers at the 60 h time point. Results in (A) and (B) are expressed as mean ± SEM (three determinations) in a typical experiment from three separate experiments performed. (**C**) Net tumor growth in nude mice injected subcutaneously with 1×10^6 SK-Mel-28 melanoma cells, scrambled control cells or the MTf/B1 cell line. The MTf/B1 cell line with low MTf expression displayed the least net tumor growth after 30 days *in vivo*. (**D**) Expression of MTf protein in MTf/B1 cells remains decreased relative to parental SK-Mel-28 cells or scrambled control cell lines after 30 days of *in vivo* growth in nude mice. (C) Results are mean ± SEM (four to nine animals) in a typical experiment from two separate experiments. (D) Results are from a typical experiment performed as two separate experiments.

the *Apod* gene was downregulated in $MTf^{-/-}$ mice compared with their wild-type littermates.

Of these genes, two were identified as transcription factors, namely *Mef2a* and *Tcf4* (70,71). The *Mef2a* transcription factor is strongly expressed in muscle tissues and is involved in fetal cardiac development, calcium-signaling and the MAP kinase pathways (70,72,73). This transcription factor is suggested to be important in cell proliferation, differentiation

and survival (74). The *Tcf4* gene product plays a role in the Wnt signaling pathway (75) and the regulation of melanocyte differentiation (76). Tcf4 is expressed at high levels in some cancers, and functional genomic investigations demonstrated that this transcription factor has a role in cell proliferation (71,77). Notably, genes such as *solute carrier family 2a member 4* (*Slc2a4*) and *Cd44* are directly regulated by Mef2a and Tcf4 (78,79), and our array data showed that *Slc2a4* and *Cd44* were affected by *MTf* deletion. In fact, *Cd44* was found in the top 30 genes showing differential regulation after *MTf* deletion (Figure 2A). These observations suggest some functional links between MTf, *Mef2a* and *Tcf4*.

The other two genes showing differential expression, namely *Gls* and *Apod,* have also been demonstrated to have a role in proliferation and encode the proteins, glutaminase and apolipoprotein D, respectively. Glutaminase has been found to be highly expressed in the mitochondria of tumor cells immediately before the maximum rate of proliferation is achieved (80–82). Conversely, apolipoprotein D inhibits cellular proliferation and is associated with transporting sterols, steroids and arachidonic acid for tissue repair (83,84). The upregulation of *Gls* and downregulation of *Apod* in the knockout mouse compared with the wild-type indicates a direct or indirect response to gene deletion and suggests some role for MTf in proliferation. Under the current experimental conditions, no defect in growth or development was obvious and a phenotype may only be observed when the mouse is exposed to an appropriate stress.

Given these results from the $MTf^{-/-}$ mouse, it should be noted that this is a normal physiological system in a whole organism, which has many existing compensatory mechanisms that may mask deletion of MTf expression. Potentially, in melanoma cells that express high levels of MTf, the function of the protein may become more evident when its expression is decreased. MTf is hyper-expressed in melanoma cells and much less so in other tumors (1,2), suggesting a cell-type-specific function. We used PTGS in human SK-Mel-28 cells and showed that MTf downregulation impaired proliferation, DNA synthesis and migration *in vitro* and decreased tumor growth *in vivo* in nude mice. This was not a clonal effect as transfection experiments performed 6 months after the initial study gave similar results. Moreover, the decrease in MTf expression and melanoma proliferation was observed with four different siRNA constructs (*see* Materials and methods), indicating that these effects could not be explained by the off-target influence of one individual siRNA.

The addition of Fe donors such as FAC or holo-Tf did not rescue the impaired proliferation of MTf/B1 cells with low MTf expression. This indicated that decreased growth of cells with low MTf expression was independent of any effect on Fe metabolism, and this was in agreement with our $MTf^{-/-}$ mouse studies and investigations *in vitro* (7,9,15,18). Further, there was no difference in Fe uptake from Tf between clones with low MTf levels and the scrambled control.

Considering the role of MTf in proliferation, it is notable that evidence from hyper-expression studies using melanoma cells suggested that increased MTf expression results in accelerated growth (85). In contrast, MTf hyper-expression in CHO cells did not increase proliferation (35). These data support our results suggesting that the role of MTf may only be obvious in melanoma cells where it is highly expressed.

Potentially, the changes in gene expression observed in the $MTf^{-/-}$ mice compared with $MTf^{+/+}$ littermates could be involved in the altered proliferation observed in the PTGS experiments using melanoma cells. Assessment of gene expression by RT–PCR indicated that in melanoma cells engineered with suppressed MTf expression, *hMEF2A* and *hTCF4* were similarly upregulated. These data support the relationship between MTf and the transcription factors observed in the $MTf^{-/-}$ mouse. Despite the decrease of *Apod* expression in $MTf^{-/-}$ mice compared with wild-type animals, there was no change in *hAPOD* expression in MTf/B1 cells compared with their scrambled control counterparts. Therefore, to rule out the possibility that decreased *Apod* expression in $MTf^{-/-}$ mice may have resulted from events associated with *MTf* gene deletion, we examined the expression of a gene at the same chromosomal locus as *MTf* and *Apod*. Indeed, *TfR1* is located on the same strand as *MTf* (714 kb apart), and the former gene showed no change in its expression when comparing $MTf^{-/-}$ and $MTf^{+/+}$ mice (9). *Apod* is located on the alternate strand as *MTf* (564 kb apart), and these latter results demonstrating no difference in *TfR1* expression between the genotypes (9) suggest that the alteration in *Apod* expression was not due to a deletion in *MTf*. However, we cannot rule out the fact that the deleted region of *MTf* itself may contain distal regulatory elements for nearby genes such as *Apod* that could affect its expression in the $MTf^{-/-}$ mouse model.

In summary, studies using $MTf^{-/-}$ mice conclusively demonstrate that MTf does not play an essential role in Fe metabolism or homeostasis. We identified differentially expressed genes such as *Mef2a, Tcf4, Gls* and *Apod* in the knockout mouse, which suggested that MTf may play a role in growth and proliferation under normal physiological conditions. We also showed using melanoma cells that MTf downregulation resulted in inhibition of proliferation and cell migration *in vitro* and reduced tumor growth *in vivo* in nude mice. These data indicate that MTf plays an important role in melanoma cell growth and tumorigenesis.

Acknowledgements

References

1. Woodbury,R.G., Brown,J.P., Yeh,M.Y., Hellstrom,I. and Hellstrom,K.E. (1980) Identification of a cell surface protein, p97, in human melanomas and certain other neoplasms. *Proc. Natl Acad. Sci. USA*, **77**, 2183–2187.
2. Brown,J.P., Woodbury,R.G., Hart,C.E., Hellstrom,I. and Hellstrom,K.E. (1981) Quantitative analysis of melanoma-associated antigen p97 in normal and neoplastic tissues. *Proc. Natl Acad. Sci. USA*, **78**, 539–543.

3. Brown,J.P., Hewick,R.M., Hellstrom,I., Hellstrom,K.E., Doolittle,R.F. and Dreyer,W.J. (1982) Human melanoma-associated antigen p97 is structurally and functionally related to transferrin. *Nature*, **296**, 171–173.

4. Sciot,R., de Vos,R., van Eyken,P., van der Steen,K., Moerman,P. and Desmet,V.J. (1989) *In situ* localization of melanotransferrin (melanoma-associated antigen P97) in human liver. A light- and electronmicroscopic immunohistochemical study. *Liver*, **9**, 110–119.

5. Alemany,R., Vila,M.R., Franci,C., Egea,G., Real,F.X. and Thomson,T.M. (1993) Glycosyl phosphatidylinositol membrane anchoring of melanotransferrin (p97): apical compartmentalization in intestinal epithelial cells. *J. Cell Sci.*, **104**, 1155–1162.

6. Rothenberger,S., Food,M.R., Gabathuler,R., Kennard,M.L., Yamada,T., Yasuhara,O., McGeer,P.L. and Jefferies,W.A. (1996) Coincident expression and distribution of melanotransferrin and transferrin receptor in human brain capillary endothelium. *Brain Res.*, **712**, 117–121.

7. Richardson,D.R. (2000) The role of the membrane-bound tumour antigen, melanotransferrin (p97), in iron uptake by the human malignant melanoma cell. *Eur. J. Biochem.*, **267**, 1290–1298.

8. Sekyere,E.O., Dunn,L.L. and Richardson,D.R. (2005) Examination of the distribution of the transferrin homologue, melanotransferrin (tumour antigen p97), in mouse and human. *Biochim. Biophys. Acta*, **1722**, 131–142.

9. Sekyere,E.O., Dunn,L.L., Suryo Rahmanto,Y. and Richardson,D.R. (2005) Role of melanotransferrin in iron metabolism: studies using targeted gene disruption in-vivo. *Blood*, **107**, 2599–2601.

10. Brown,J.P., Nishiyama,K., Hellstrom,I. and Hellstrom,K.E. (1981) Structural characterization of human melanoma-associated antigen p97 with monoclonal antibodies. *J. Immunol.*, **127**, 539–546.

11. Rose,T.M., Plowman,G.D., Teplow,D.B., Dreyer,W.J., Hellstrom,K.E. and Brown,J.P. (1986) Primary structure of the human melanoma-associated antigen p97 (melanotransferrin) deduced from the mRNA sequence. *Proc. Natl Acad. Sci. USA*, **83**, 1261–1265.

12. Plowman,G.D., Brown,J.P., Enns,C.A., Schroder,J., Nikinmaa,B., Sussman,H.H., Hellstrom,K.E. and Hellstrom,I. (1983) Assignment of the gene for human melanoma-associated antigen p97 to chromosome 3. *Nature*, **303**, 70–72.

13. Baker,E.N., Baker,H.M., Smith,C.A., Stebbins,M.R., Kahn,M., Hellstrom,K.E. and Hellstrom,I. (1992) Human melanotransferrin (p97) has only one functional iron-binding site. *FEBS Lett.*, **298**, 215–218.

14. Richardson,D.R. and Baker,E. (1990) The uptake of iron and transferrin by the human malignant melanoma cell. *Biochim. Biophys. Acta*, **1053**, 1–12.

15. Richardson,D.R. and Baker,E. (1991) The release of iron and transferrin from the human melanoma cell. *Biochim. Biophys. Acta*, **1091**, 294–302.

16. Kennard,M.L., Feldman,H., Yamada,T. and Jefferies,W.A. (1996) Serum levels of the iron binding protein p97 are elevated in Alzheimer's disease. *Nat. Med.*, **2**, 1230–1235.

17. Kim,D.K., Seo,M.Y., Lim,S.W., Kim,S., Kim,J.W., Carroll,B.J., Kwon,D.Y., Kwon,T. and Kang,S.S. (2001) Serum melanotransferrin, p97 as a biochemical marker of Alzheimer's disease. *Neuropsychopharmacology*, **25**, 84–90.

18. Richardson,D. and Baker,E. (1991) The uptake of inorganic iron complexes by human melanoma cells. *Biochim. Biophys. Acta*, **1093**, 20–28.

19. Food,M.R., Sekyere,E.O. and Richardson,D.R. (2002) The soluble form of the membrane-bound transferrin homologue, melanotransferrin, inefficiently donates iron to cells via nonspecific internalization and degradation of the protein. *Eur. J. Biochem.*, **269**, 4435–4445.

20. Kawabata,H., Tong,X., Kawanami,T., Wano,Y., Hirose,Y., Sugai,S. and Koeffler,H.P. (2004) Analyses for binding of the transferrin family of proteins to the transferrin receptor 2. *Br. J. Haematol.*, **127**, 464–473.

21. Demeule,M., Poirier,J., Jodoin,J. *et al.* (2002) High transcytosis of melanotransferrin (P97) across the blood-brain barrier. *J. Neurochem.*, **83**, 924–933.

22. Moroo,I., Ujiie,M., Walker,B.L., Tiong,J.W., Vitalis,T.Z., Karkan,D., Gabathuler,R., Moise,A.R. and Jefferies,W.A. (2003) Identification of a novel route of iron transcytosis across the mammalian blood–brain barrier. *Microcirculation*, **10**, 457–462.

23. Jefferies,W.A., Food,M.R., Gabathuler,R., Rothenberger,S., Yamada,T., Yasuhara,O. and McGeer,P.L. (1996) Reactive microglia specifically associated with amyloid plaques in Alzheimer's disease brain tissue express melanotransferrin. *Brain Res.*, **712**, 122–126.

24. McNagny,K.M., Rossi,F., Smith,G. and Graf,T. (1996) The eosinophil-specific cell surface antigen, EOS47, is a chicken homologue of the oncofetal antigen melanotransferrin. *Blood*, **87**, 1343–1352.

25. Nakamasu,K., Kawamoto,T., Shen,M., Gotoh,O., Teramoto,M., Noshiro,M. and Kato,Y. (1999) Membrane-bound transferrin-like protein (MTf): structure, evolution and selective expression during chondrogenic differentiation of mouse embryonic cells. *Biochim. Biophys. Acta*, **1447**, 258–264.

26. Kato,Y., Matsukawa,H., Yoshiwara,Y., Oka,O. and Fujita,T. (2001) Method and reagent for assaying arthritis-associated melanotransferrin. *International Publication no. WO 01/11368*.

27. Sala,R., Jefferies,W.A., Walker,B. *et al.* (2002) The human melanoma associated protein melanotransferrin promotes endothelial cell migration and angiogenesis *in vivo*. *Eur. J. Cell Biol.*, **81**, 599–607.

28. Demeule,M., Bertrand,Y., Michaud-Levesque,J., Jodoin,J., Rolland,Y., Gabathuler,R. and Beliveau,R. (2003) Regulation of plasminogen activation: a role for melanotransferrin (p97) in cell migration. *Blood*, **102**, 1723–1731.

29. Kingston,H. and Jassie,L. (eds.) (1988) *Introduction to Microwave Sample Preparation. Theory and Practice*. American Chemical Society, Washington, DC.

30. Lonnstedt,I. and Speed,T. (2002) Replicated microarray data. *Statistica Sinica*, **12**, 31–46.

31. Holm,S. (1979) A simple sequentially rejective multiple test procedure. *Scand J. Stat.*, **6**, 65–70.

32. Le,N.T. and Richardson,D.R. (2004) Iron chelators with high antiproliferative activity up-regulate the expression of a growth inhibitory and metastasis suppressor gene: a link between iron metabolism and proliferation. *Blood*, **104**, 2967–2975.

33. Gao,J. and Richardson,D.R. (2001) The potential of iron chelators of the pyridoxal isonicotinoyl hydrazone class as effective antiproliferative agents, IV: the mechanisms involved in inhibiting cell-cycle progression. *Blood*, **98**, 842–850.

34. Richardson,D. and Baker,E. (1992) Two mechanisms of iron uptake from transferrin by melanoma cells. The effect of desferrioxamine and ferric ammonium citrate. *J. Biol. Chem.*, **267**, 13972–13979.

35. Kennard,M.L., Richardson,D.R., Gabathuler,R., Ponka,P. and Jefferies,W.A. (1995) A novel iron uptake mechanism mediated by GPI-anchored human p97. *EMBO J.*, **14**, 4178–4186.

36. Richardson,D., Ponka,P. and Baker,E. (1994) The effect of the iron(III) chelator, desferrioxamine, on iron and transferrin uptake by the human malignant melanoma cell. *Cancer Res.*, **54**, 685–689.

37. Gordon-Thomson,C., Jones,J., Mason,R.S. and Moore,G.P. (2005) ErbB receptors mediate both migratory and proliferative activities in human melanocytes and melanoma cells. *Melanoma Res.*, **15**, 21–28.

38. Sossey-Alaoui,K., Li,X., Ranalli,T.A. and Cowell,J.K. (2005) WAVE3-mediated cell migration and lamellipodia formation are regulated downstream of phosphatidylinositol 3-kinase. *J. Biol. Chem.*, **280**, 21748–21755.

39. Balsari,A., Tortoreto,M., Besusso,D., Petrangolini,G., Sfondrini,L., Maggi,R., Menard,S. and Pratesi,G. (2004) Combination of a CpG-oligodeoxynucleotide and a topoisomerase I inhibitor in the therapy of human tumour xenografts. *Eur. J. Cancer*, **40**, 1275–1281.

40. Sekyere,E. and Richardson,D.R. (2000) The membrane-bound transferrin homologue melanotransferrin: roles other than iron transport? *FEBS Lett.*, **483**, 11–16.

41. Miczek,K.A., Weerts,E., Haney,M. and Tidey,J. (1994) Neurobiological mechanisms controlling aggression: preclinical developments for pharmacotherapeutic interventions. *Neurosci. Biobehav. Rev.*, **18**, 97–110.

42. Crawley,J.N. (2003) Behavioral phenotyping of rodents. *Comp. Med.*, **53**, 140–146.

43. Crawley,J.N. (1999) Behavioral phenotyping of transgenic and knockout mice: experimental design and evaluation of general health, sensory functions, motor abilities, and specific behavioral tests. *Brain Res.*, **835**, 18–26.

44. Beliveau,R. (2003) Vectorization of proteins across the blood–brain barrier: high transcytosis of melanotransferrin (P97). *J. Neurochem.*, **85**, 7–7.

45. Olfert,E.D., Cross,B.M. and McWilliam,S.S. (1993) *Guide to the Care and Use of Experimental Animals*. Canadian Council on Animal Care, Ottawa.

46. Taconic (2004) Taconic Technical Library: Taconic B6 Phenotyping. Taconic, vol. 2005.

47. Sproule,T.J., Jazwinska,E.C., Britton,R.S., Bacon,B.R., Fleming,R.E., Sly,W.S. and Roopenian,D.C. (2001) Naturally variant autosomal and sex-linked loci determine the severity of iron overload in beta 2-microglobulin-deficient mice. *Proc. Natl Acad. Sci. USA*, **98**, 5170–5174.

48. Krijt,J., Cmejla,R., Sykora,V., Vokurka,M., Vyoral,D. and Necas,E. (2004) Different expression pattern of hepcidin genes in the liver and pancreas of C57BL/6N and DBA/2N mice. *J. Hepatol.*, **40**, 891–896.
49. Morgan,E.H. (1981) Transferrin: biochemistry, physiology and clinical significance. *Mol. Aspects Med.*, **4**, 1–123.
50. Desrosiers,R.R., Bertrand,Y., Nguyen,Q.T., Demeule,M., Gabathuler,R., Kennard,M.L., Gauthier,S. and Beliveau,R. (2003) Expression of melanotransferrin isoforms in human serum: relevance to Alzheimer's disease. *Biochem. J.*, **374**, 463–471.
51. Bridge,A.J., Pebernard,S., Ducraux,A., Nicoulaz,A.L. and Iggo,R. (2003) Induction of an interferon response by RNAi vectors in mammalian cells. *Nat. Genet.*, **34**, 263–264.
52. Lambert,L.A., Perri,H. and Meehan,T.J. (2005) Evolution of duplications in the transferrin family of proteins. *Comp. Biochem. Physiol. B. Biochem. Mol. Biol.*, **140**, 11–25.
53. Goto,Y., Paterson,M. and Listowsky,I. (1983) Iron uptake and regulation of ferritin synthesis by hepatoma cells in hormone-supplemented serum-free media. *J. Biol. Chem.*, **258**, 5248–5255.
54. Michaud-Levesque,J., Rolland,Y., Demeule,M., Bertrand,Y. and Beliveau,R. (2005) Inhibition of endothelial cell movement and tubulogenesis by human recombinant soluble melanotransferrin: involvement of the u-PAR/LRP plasminolytic system. *Biochim. Biophys. Acta*, **1743**, 243–253.
55. Richardson,D.R. and Morgan,E.H. (2004) The transferrin homologue, melanotransferrin (p97), is rapidly catabolized by the liver of the rat and does not effectively donate iron to the brain. *Biochim. Biophys. Acta*, **1690**, 124–133.
56. Pan,W., Kastin,A.J., Zankel,T.C., van Kerkhof,P., Terasaki,T. and Bu,G. (2004) Efficient transfer of receptor-associated protein (RAP) across the blood–brain barrier. *J. Cell. Sci.*, **117**, 5071–5078.
57. Ward,P.P., Mendoza-Meneses,M., Cunningham,G.A. and Conneely,O.M. (2003) Iron status in mice carrying a targeted disruption of lactoferrin. *Mol. Cell. Biol.*, **23**, 178–185.
58. Fleming,M.D., Romano,M.A., Su,M.A., Garrick,L.M., Garrick,M.D. and Andrews,N.C. (1998) Nramp2 is mutated in the anemic Belgrade (b) rat: evidence of a role for Nramp2 in endosomal iron transport. *Proc. Natl Acad. Sci. USA*, **95**, 1148–1153.
59. Levy,J.E., Jin,O., Fujiwara,Y., Kuo,F. and Andrews,N.C. (1999) Transferrin receptor is necessary for development of erythrocytes and the nervous system. *Nat. Genet.*, **21**, 396–399.
60. Wallace,D.F., Summerville,L., Lusby,P.E. and Subramaniam,V.N. (2005) First phenotypic description of transferrin receptor 2 knockout mouse, and the role of hepcidin. *Gut*, **54**, 980–986.
61. Zhou,X.Y., Tomatsu,S., Fleming,R.E. *et al.* (1998) *HFE* gene knockout produces mouse model of hereditary hemochromatosis. *Proc. Natl Acad. Sci. USA*, **95**, 2492–2497.
62. Meyron-Holtz,E.G., Ghosh,M.C., Iwai,K. *et al.* (2004) Genetic ablations of iron regulatory proteins 1 and 2 reveal why iron regulatory protein 2 dominates iron homeostasis. *EMBO J.*, **23**, 386–395.
63. Trenor,C.C. III, Campagna,D.R., Sellers,V.M., Andrews,N.C. and Fleming,M.D. (2000) The molecular defect in hypotransferrinemic mice. *Blood*, **96**, 1113–1118.
64. Kriegerbeckova,K. and Kovar,J. (2000) Role of melanotransferrin (p97) in non-transferrin iron uptake by HeLa and K562 cells. *Folia Biol. (Praha)*, **46**, 77–81.
65. Neckers,L.M. and Cossman,J. (1983) Transferrin receptor induction in mitogen-stimulated human T lymphocytes is required for DNA synthesis and cell division and is regulated by interleukin 2. *Proc. Natl Acad. Sci. USA*, **80**, 3494–3498.
66. Kameyama,K., Takezaki,S., Kanzaki,T. and Nishiyama,S. (1986) HLA-DR and melanoma-associated antigen (p97) expression during the cell cycle in human melanoma cell lines, and the effects of recombinant gamma-interferon: two-color flow cytometric analysis. *J. Invest. Dermatol.*, **87**, 313–318.
67. Seligman,P.A., Butler,C.D., Massey,E.J., Kaur,J.A., Brown,J.P., Plowman,G.D., Miller,Y. and Jones,C. (1986) The p97 antigen is mapped to the q24-qter region of chromosome 3; the same region as the transferrin receptor. *Am. J. Hum. Genet.*, **38**, 540–548.
68. Beard,J.L., Connor,J.R. and Jones,B.C. (1993) Iron in the brain. *Nutr. Rev.*, **51**, 157–170.
69. Richardson,D.R. and Ponka,P. (1997) The molecular mechanisms of the metabolism and transport of iron in normal and neoplastic cells. *Biochim. Biophys. Acta*, **1331**, 1–40.
70. Black,B.L. and Olson,E.N. (1998) Transcriptional control of muscle development by myocyte enhancer factor-2 (MEF2) proteins. *Annu. Rev. Cell Dev. Biol.*, **14**, 167–196.
71. Mann,B., Gelos,M., Siedow,A. *et al.* (1999) Target genes of beta-catenin-T-cell factor/lymphoid-enhancer-factor signaling in human colorectal carcinomas. *Proc. Natl Acad. Sci. USA*, **96**, 1603–1608.
72. Zhao,M., New,L., Kravchenko,V.V., Kato,Y., Gram,H., di Padova,F., Olson,E.N., Ulevitch,R.J. and Han,J. (1999) Regulation of the MEF2 family of transcription factors by p38. *Mol. Cell. Biol.*, **19**, 21–30.
73. Naya,F.J., Black,B.L., Wu,H., Bassel-Duby,R., Richardson,J.A., Hill,J.A. and Olson,E.N. (2002) Mitochondrial deficiency and cardiac sudden death in mice lacking the MEF2A transcription factor. *Nat. Med.*, **8**, 1303–1309.
74. McKinsey,T.A., Zhang,C.L. and Olson,E.N. (2002) MEF2: a calcium-dependent regulator of cell division, differentiation and death. *Trends Biochem. Sci.*, **27**, 40–47.
75. Graham,T.A., Ferkey,D.M., Mao,F., Kimelman,D. and Xu,W. (2001) Tcf4 can specifically recognize beta-catenin using alternative conformations. *Nat. Struct. Biol.*, **8**, 1048–1052.
76. Furumura,M., Potterf,S.B., Toyofuku,K., Matsunaga,J., Muller,J. and Hearing,V.J. (2001) Involvement of ITF2 in the transcriptional regulation of melanogenic genes. *J. Biol. Chem.*, **276**, 28147–28154.
77. Zhao,D.H., Hong,J.J., Guo,S.Y., Yang,R.L., Yuan,J., Wen,C.Y., Zhou,K.Y. and Li,C.J. (2004) Aberrant expression and function of TCF4 in the proliferation of hepatocellular carcinoma cell line BEL-7402. *Cell Res.*, **14**, 74–80.
78. Thai,M.V., Guruswamy,S., Cao,K.T., Pessin,J.E. and Olson,A.L. (1998) Myocyte enhancer factor 2 (MEF2)-binding site is required for GLUT4 gene expression in transgenic mice. Regulation of MEF2 DNA binding activity in insulin-deficient diabetes. *J. Biol. Chem.*, **273**, 14285–14292.
79. Wielenga,V.J., Smits,R., Korinek,V., Smit,L., Kielman,M., Fodde,R., Clevers,H. and Pals,S.T. (1999) Expression of CD44 in Apc and Tcf mutant mice implies regulation by the WNT pathway. *Am. J. Pathol.*, **154**, 515–523.
80. Medina,M.A., Sanchez-Jimenez,F., Marquez,J., Rodriguez Quesada,A. and Nunez de Castro,I. (1992) Relevance of glutamine metabolism to tumor cell growth. *Mol. Cell. Biochem.*, **113**, 1–15.
81. Aledo,J.C., Segura,J.A., Medina,M.A., Alonso,F.J., Nunez de Castro,I. and Marquez,J. (1994) Phosphate-activated glutaminase expression during tumor development. *FEBS Lett.*, **341**, 39–42.
82. Kvamme,E., Roberg,B. and Torgner,I.A. (2000) Phosphate-activated glutaminase and mitochondrial glutamine transport in the brain. *Neurochem. Res.*, **25**, 1407–1419.
83. Terrisse,L., Poirier,J., Bertrand,P., Merched,A., Visvikis,S., Siest,G., Milne,R. and Rassart,E. (1998) Increased levels of apolipoprotein D in cerebrospinal fluid and hippocampus of Alzheimer's patients. *J. Neurochem.*, **71**, 1643–1650.
84. Sugimoto,K., Simard,J., Haagensen,D.E. and Labrie,F. (1994) Inverse relationships between cell proliferation and basal or androgen-stimulated apolipoprotein D secretion in LNCaP human prostate cancer cells. *J. Steroid Biochem. Mol. Biol.*, **51**, 167–174.
85. Estin,C.D., Stevenson,U., Kahn,M., Hellstrom,I. and Hellstrom,K.E. (1989) Transfected mouse melanoma lines that express various levels of human melanoma-associated antigen p97. *J. Natl Cancer Inst.*, **81**, 445–448.